Journal of Fluorescence, Vol. 12, No. 1, March 2002 (© 2002)

Study of Preferential Solvation in Binary Mixtures by Means of Frequency-Domain Fluorescence Spectroscopy

N. Kh. Petrov,[1] D. E. Markov,[1] M. N. Gulakov,[1] M. V. Alfimov,[1] and H. Staerk[2,3]

Received July 24,2001; revised October 26, 2001; accepted October 26, 2001

The preferential solvation of 8-*N*,*N*-(dimethylamino)-11H-indeno[2,1-a]pyrene, Py(S)DMA, in its transient charge transfer (CT) state in binary solvents such as toluene/DMSO liquid mixtures was studied by means of frequency-domain fluorometry. The data obtained were considered within the following kinetic scheme: the preferential solvation was described by the system of consecutive reversible reactions of which each step is associated with the absorption of one DMSO molecule in the first solvation shell of the fluoresent Py(S)DMA dipolar CT molecule. The rate constants of the first two reversible elementary processes (i.e., the decay of solvation complexes of Py(S)DMA with one and two polar molecules, $k_{-1} = 1.1\ 10^9\ s^{-1}$ and $k_{-2} = 1.4\ 10^9\ s^{-1}$) were determined.

KEY WORDS: Preferential solvation; frequency-domain fluorometry.

INTRODUCTION

The study of preferential solvation is of interest for obtaining deeper insight into the general mechanism of the influence of solvents on chemical reactions [1]. The currently available methods of time-resolved optical spectroscopy, in particular the streak-camera technique [2,3], allow the study of preferential solvation by observing solvatochromic shifts of fluorescence in *binary* solvents on a picosecond time scale. Generally, the interpretation of such experimental data requires an earlier assumption of a solute-solvent interaction that, for non-specific interactions, is based usually on the Onsager model, which is suitable for binary liquid mixtures [2b]. Unlike the streak-camera technique, the phase modulation method, which had almost fallen into disrepute during the last decades [4] (after the advent of lasers in chemistry) and expanded only in the recent years [5,6], allows, in principle, the obtaining of experimental data directly in terms of rate constants of the system studied. The phase modulation method can be regarded as complementary to other methods.

The purpose of this work is to demonstrate that frequency-domain fluorescence spectroscopy is a useful tool in study of the kinetics of preferential solvation in binary mixtures. As an example, the fluorescence probe 8-*N*,*N*-(dimethylamino)-11H-indeno[2,1-a]pyrene, (Py(S)DMA), whose chemical structural formula is shown in Fig. 1, was used in toluene/DMSO mixtures (i.e., the system that had already been studied earlier by means of the spectro-streak technique [2]).

EXPERIMENTAL

The solvents used in this work, toluene and dimethylsulfoxide (DMSO), were of spectroscopic grade. The concentration of the Py(S)DMA probe in the quartz cuvettes was about $3 \cdot 10^{-5}$ mol 1^{-1}. All samples were

[1] Photochemistry Center, Russian Academy of Sciences, 117421 Moscow, Russia.
[2] Max-Planck Institut für biophysikalische Chemie, Abteilung Spektroskopie und Photochemische Kinetik, Am Fassberg, 37077 Göttingen, Germany.
[3] To whom correspondence should be addressed. Tel.: +49-551-201 1265; fax: +49-551 201 1501; e-mail: hstaerk@gwdg.de, or npetrov@photonics.ru

1053-0509/02/0300-0019/0

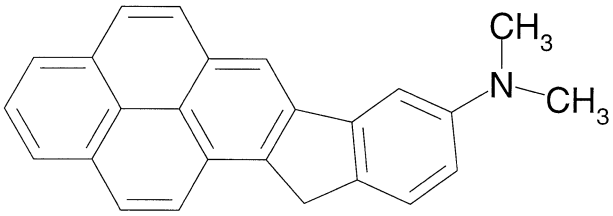

Fig. 1. The chemical structural formula of Py(S)DMA.

bubbled with argon for 15 minutes to remove oxygen from the solutions and then measured at 23°C.

Steady-state and frequency-domain fluorescence data were obtained by means of a Fluorolog-3τ spectrofluorometer (Jobin Yvon-Spex, France) with DataMax driving software. Typically, measurements were done at 14 different modulation frequencies, from 5–100 MHz at various emission wavelengths. An aqueous solution of Ludox was used as a scattering standard. The time-correlated single-photon counting method was also used for lifetime measurements on a Fluotime 200 fluorometer (PicoQuant, Germany) with FluoFit data analysis software.

The Fourier transform links the time-domain fluorescence response to a delta-function excitation—the response that is usually approximated by a sum of exponentials—with the frequency-domain response to periodically modulated excitation light. The latter response is derived from experimentally measured phase delays and modulation depths of the fluorescence signal at various modulation frequencies. So, both time-domain and frequency-domain approaches are, in principle, equivalent (for details see Ref. 5,6).

RESULTS AND DISCUSSION

First, a kinetic model of preferential solvation of an excited dipolar molecule was used for evaluating the obtained results. Currently the following kinetic model is widely accepted [2,3]. After excitation of the probe molecule, an excited charge-transfer (CT) state with a large dipole moment is reached by photoinduced intramolecular electron transfer. Then a fast reorientation (on the subpicosecond time scale) of surrounding dipolar solvent molecules occurs and the system reaches its first quasi-equilibrium state. After this very rapid orientational relaxation, preferential solvation takes place and, as a result, the system relaxes to its final equilibrium state. This latter process is relatively slow and is associated with the diffusion transport of polar molecules from the bulk into the solvation shell of the excited dipole [3a,7]. During this diffusion transport, non-polar component molecules may be regarded as an inert medium. The number of solvating polar molecules (i.e., the solvation number) depends on the (volume) fraction of the polar solvent component.

Particularly with Py(S)DMA, the excited probe rapidly reaches the excited CT state with a large dipole moment ($\mu \sim 20$ D) that ensures a large dipole-dipole interaction between the probe molecule and the polar solvent component of the solution (e.g., DMSO, $\mu \sim 4$ D). Compared with the long CT fluorescence lifetime in the range of 24–30 ns, the duration of establishing a steady-state dielectric enrichment around the excited CT dipole is short.

Thus the preferential solvation of an excited CT dipole in binary mixtures can be described by the system of consecutive reversible reactions, of which each step is associated with the absorption of one polar molecule in the first solvation shell of the dipolar CT molecule (this is quite similar to the model suggested in [3a]). In the scheme shown in Fig. 2, **A** is a polar-component molecule of a binary solvent; **B** is the ground state and **B*** the excited state of a dipolar CT probe molecule; **B*A, B*A$_2$** are the complexes of the latter after absorbtion of one or two polar molecules from the bulk, respectively.

Pseudo–first-order rate constants k_1, k_2, and k_3 describe diffusion transport of polar molecules into the first solvation shell of **B**. Note that $k_i \approx k_d$ [**A**] ($i = 1, 2, 3 \ldots$), where [**A**] $\approx$ [**A**]$_0$; k_d, the bimolecular diffusion-limited rate-constant, mainly determined by the viscosity of the non-polar component, that is, toluene. As mentioned above, a diffusion type of solvation shell creation is now widely accepted.

Molecules **A** can escape the solvent shell of the dipolar molecule. This process is described by the first-order rate constants k_{-i} ($i = 1, 2, \ldots$ n). It should be mentioned that so far only little has been known about the decay rates of solvation complexes.

Γ_i is the rate constant of fluorescence deactivation of different solvated states. These rate constants are supposed to be much smaller than those that describe the creation and decay of the solvation shell. Because the excited states (i.e., **B*, B*A, B*A$_2$**, . . .) are different in terms of energy, they can, in principle, be separated by

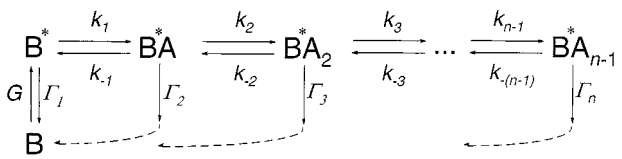

Fig. 2. The kinetic scheme of preferential solvation of the excited dipolar molecule in binary mixtures (see explanation in the text).

observing the fluorescence in corresponding spectral bands.

Note that the solvation number of polar molecules in the first solvation shell of the excited dipolar solute can be determined only on average. As shown by a computer simulation of preferential solvation of the coumarin 135 solute molecule in mixtures of methanol and hexane [3b], there might exist a quite broad distribution of solvation numbers of the excited dipolar molecule. So, the total process is described by "chains" of the consecutive reactions of various lengths that occur concomitantly. The fluorescence intensity detected at a certain spectral band is, therefore, a superposition of emissions of solute-solvent complexes of different compositions. Obviously this makes a quantitative interpretation of experimental data more difficult.

As to experimental results, Fig. 3 shows that on increasing the volume fraction of DMSO, Stokes' shifts of the CT fluorescence peaks of Py(S)DMA occur while the fluorescence intensity decreases. Fig. 4 demonstrates that spectral shifts of the CT fluorescence peak of Py(S)-DMA, with respect to the fluorescence peak in neat toluene as a function of the volume fraction of DMSO, has a clear-cut saturation feature when the concentration of the polar component increases. This saturation is attributed to the existence of a limited number of polar solvent molecules in the first solvation shell of the excited dipolar molecule [8]. Moreover, recent streak-camera studies [2c] have shown that at equilibrium the solvation shell on average comprises only a few DMSO molecules for small-volume fractions of the polar solvent component. For example, the solvation number is approximately 2 for a DMSO fraction of 3 vol.%. As described below, this facilitates the achievement of detailed information

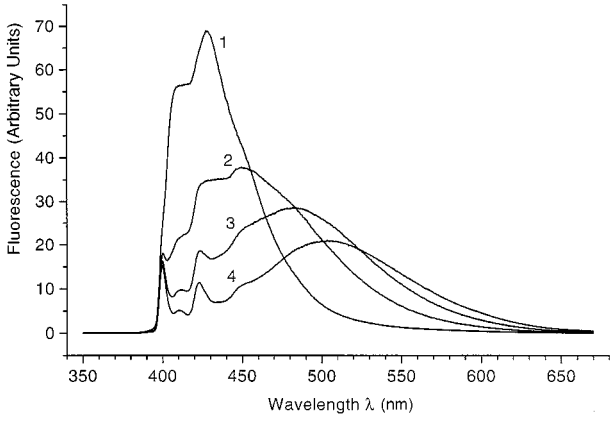

Fig. 3. Fluorescence spectra of Py(S)DMA solutions in neat toluene (1), and in toluene/DMSO mixtures: 1.6 vol.% DMSO (2); 3.2 vol.% DMSO (3); 6.3 vol.% DMSO (4). Excitation wavelength, 337 nm.

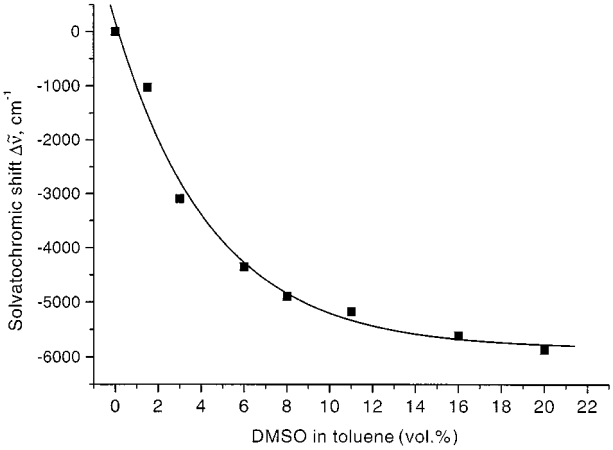

Fig. 4. The plot of solvatochromic shift for the Py(S)DMA fluorescence peak versus the volume fraction DMSO in mixtures with toluene with respect to neat toluene. The negative sign corresponds to the shift of fluorescence peak to lower energies.

about the kinetics of preferential solvation by means of the frequency-domain methods.

Typical plots of fluorescence phase delays relative to the excitation light versus wavelength of the Py(S)DMA fluorescence are shown in Fig. 5 for some volume fractions of DMSO and neat toluene. For the latter, the phase delay is almost constant in the range from 400–500 nm. Upon increasing the volume fraction of DMSO in binary mixtures, the phase delay decreases in a spectral band around 420 nm and concomitantly increases for wavelengths longer than 460 nm. Using an empirical rule—the longer the lifetime, the larger the phase delay—one might conclude that these experimental results qualitatively are

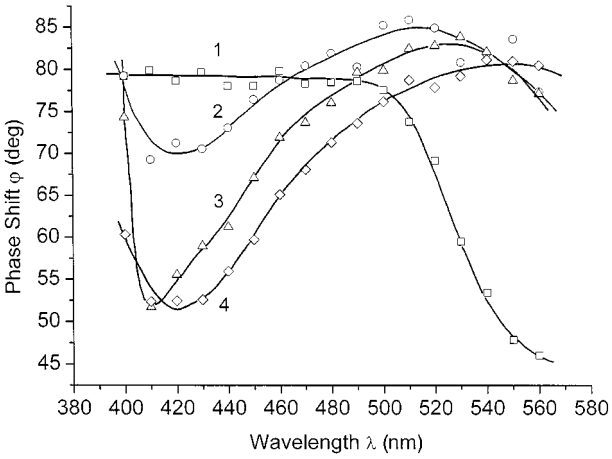

Fig. 5. The plot of phase delays of fluorescence versus the emission wavelength at a 40-MHz molulation frequency for neat toluene (1); and toluene/DMSO mixtures: 1.6 vol.% DMSO (2); 3.2 vol.% DMSO (3); 6.3 vol.% DMSO (4).

in agreement with the kinetic scheme (see Fig. 2). Notably, the pioneer work by Cherkasov and coworkers [9] had anticipated the main features of applications of frequency-domain fluorometry to preferential solvation that was further developed by Lakowicz [6a,b].

Lifetime measurements, carried out under the same conditions by the time-correlated single-photon counting method, have corroborated the time scale of the above results. For all mixtures studied, the fluorescence decay in the range of 410–440 nm fits to two exponential functions of a short lifetime of ca. 0.6 ns and of a long lifetime that varies from 24–29 ns for DMSO volume fractions 1.6–6.25 vol.%. The long lifetime obviously corresponds to the fluorescence transition from **B*** to the ground state, whereas the short lifetime component is associated with the formation of the complex **B*A** (see Fig. 2). The fluorescence decay in the long-wavelength region (ca. 550 nm) can always be fitted by a single exponential function with a characteristic time of ca. 29 ns. In neat solvents, there is only a single decay-time independent of emission wavelengths: in toluene this is 20 ns, and in chlorobenzene, 22 ns. The dielectric constant of chlorobenzene is 5.6, which corresponds to that of a 4-vol.% DMSO mixture with toluene. As expected, the procedure of frequency-domain data analysis, mentioned above, gives approximately the same lifetimes of Py(S)DMA fluorescence for these neat and binary solvents. On the other hand, kinetic interpretation of the obtained data is difficult, or rather impossible, with the multiple-exponential fitting procedure. Therefore we approach the problem on the basis of the known kinetic scheme of preferential solvation (see Fig. 2).

The differential equations corresponding to the scheme are:

$$\left.\begin{aligned}
\frac{d}{dt}c_1(t) &= -(k_1+\Gamma_1)\,c_1(t) + k_{-1}c_2(t) + G,\\
\frac{d}{dt}c_2(t) &= k_1c_1(t) - (k_{-1}+k_2+\Gamma_2)\,c_2(t) + k_{-2}c_3(t),\\
&\vdots\\
\frac{d}{dt}c_j(t) &= k_{j-1}c_{j-1}(t) - (k_{-(j-1)}+k_j+\Gamma_j)\,c_j(t)\\
&\quad + k_{-j}c_{j+1}(t),\\
&\vdots\\
\frac{\mathrm{d}}{dt}c_n(t) &= k_{n-1}c_{n-1}(t) - (k_{-(n-1)}+\Gamma_n)\,c_n(t),
\end{aligned}\right\} \tag{1}$$

where $c_j(t)$ ($j = 1, 2, 3, \ldots, n$) are the concentrations of **B*, B*A, B*A$_2$**, . . . , **B*A$_n$** at time t, respectively. On a harmonic excitation $G = G_0e^{i\omega t}$, where ω is the modulation angular frequency of the excitation light (i.e., $\omega = 2\pi f$, where f is the modulation frequency in Hz) and $i^2 = -1$, each concentration is $c_j(t) = \tilde{C}_j e^{i\omega t}$. Here $\tilde{C}_j$ are the complex functions of the angular frequency. Substituting these into Eq. (1), we obtain:

$$\left.\begin{aligned}
i\omega\,\tilde{C}_1 &= -(k_1+\Gamma_1)\,\tilde{C}_1 + k_{-1}\tilde{C}_2 + G_0,\\
i\omega\,\tilde{C}_2 &= k_1\tilde{C}_1 - (k_{-1}+k_2+\Gamma_2)\,\tilde{C}_2 + k_{-2}\tilde{C}_3,\\
&\vdots\\
i\omega\,\tilde{C}_j &= k_{j-1}\tilde{C}_{j-1} - (k_{-(j-1)}+k_j+\Gamma_j)\,\tilde{C}_j + k_{-j}\tilde{C}_{j+1},\\
&\vdots\\
i\omega\,\tilde{C}_n &= k_{n-1}\tilde{C}_{n-1} - (k_{-(n-1)}+\Gamma_n)\tilde{C}_n
\end{aligned}\right\} \tag{2}$$

Following the method of continued fractions, used by Morita [10] in a similar situation, we obtain from Eq. (2):

$$\tilde{C}_1 = \frac{G_0}{i\omega + k_1 + \Gamma_1 - k_{-1}\dfrac{\tilde{C}_2}{\tilde{C}_1}}, \tag{3}$$

$$\frac{\tilde{C}_j}{\tilde{C}_{j-1}} = \frac{k_{j-1}}{i\omega + k_j + \Gamma_j + k_{-(j-1)} - k_{-j}\dfrac{\tilde{C}_{j+1}}{\tilde{C}_j}}, \tag{4}$$

$$\frac{\tilde{C}_n}{\tilde{C}_{n-1}} = \frac{k_{n-1}}{i\omega + \Gamma_n + k_{-(n-1)}}. \tag{5}$$

From Eqs. (3–5) the explicit formula for each complex concentration $\tilde{C}_j$ can be obtained.

For example, for $n = 1$, and 2:

$$\tilde{C}_1^{(1)} = \frac{G_0}{i\omega + k_1 + \Gamma_1}, \tag{6}$$

$$\tilde{C}_1^{(2)} = \frac{G_0}{i\omega + k_1 + \Gamma_1 - \dfrac{k_1k_{-1}}{i\omega + k_{-1} + \Gamma_2}}, \tag{7}$$

$$\tilde{C}_2^{(2)} = \frac{k_1}{i\omega + k_{-1} + \Gamma_2} \times \frac{G_0}{i\omega + k_1 + \Gamma_1 - \dfrac{k_1k_{-1}}{i\omega + k_{-1} + \Gamma_2}}. \tag{8}$$

The complex concentration can be given as $\tilde{C}_j = z_jG_0$, where the complex number $z_j = P_j(\omega) + iQ_j(\omega)$. Bearing in mind that multiplication of the complex numbers means multiplication of their moduli and addition of the phase angles, the phase delay φ_j, with respect to excitation, is determined as:

$$\tan\varphi_j = -Q_j(\omega)/P_j(\omega) \tag{9}$$

and the modulation coefficient as:

$$m_j = \sqrt{P_j^2 + Q_j^2} \tag{10}$$

Note that the imaginary part of G_0 is equal to zero, and hence its phase angle is zero too.

In a system with one excited state, which corresponds to a neat solvent, one can derive easily from equation (6) the well-known explicit expressions for the phase delay of emission φ relative to a periodically modulated excitation light and a modulation depth *m* (see, for example, [4]):

$$\tan \varphi = \omega/\Gamma_1, \qquad m = (1 + (\omega/\Gamma_1)^2)^{-1/2} \tag{11}$$

where ω is the angular frequency of modulation.

For more complex systems with two excited states, (e.g., **B*, B*A**), the far more intricate expressions follow from equations (7,8) [6b]:

$$\left.\begin{aligned} \tan \varphi_1 &= \frac{\omega(\alpha\gamma - \beta + \omega^2)}{\alpha\omega^2 + (\beta - \omega^2)\gamma}, \\ m_1 &= \frac{\beta}{\gamma} \cdot \left[\frac{\gamma^2 + \omega^2}{(\beta - \omega^2)^2 + \alpha^2\omega^2}\right]^{\frac{1}{2}}, \\ \tan \varphi_2 &= \frac{\alpha\omega}{\beta - \omega^2}, \\ m_2 &= \frac{\beta}{[(\beta - \omega^2)^2 + \alpha^2\omega^2]^{\frac{1}{2}}}, \end{aligned}\right\} \tag{12}$$

where φ_1, φ_2 and m_1, m_2 are the phase delay and the modulation depth for the excited states **B*** and **B*A**, respectively; $\alpha = \Gamma_1 + \Gamma_2 + k_1 + k_{-1}$, $\beta = \Gamma_1\Gamma_2 + \Gamma_2 k_1 + \Gamma_1 k_{-1}$, $\gamma = \Gamma_2 + k_{-1}$. In the case of three excited states (i.e., **B*, B*A, B*A$_2$**), explicit expressions corresponding to Eq. (12) can be also derived, but they are too complex to be used in the fitting procedure.

However, a more important result can be derived from Eq. (5); that is, for any kinetic scheme the phase difference between the last two adjacent states is:

$$\tan(\varphi_n - \varphi_{(n-1)}) = \frac{\omega}{\Gamma_n + k_{-(n-1)}} \tag{13}$$

This illustrates the general rule, first suggested by Weber [11], that expressions for differential phase angles between the states might be simpler and more useful in analysis. The linear dependence of the tangent of the phase difference on the angular frequency of modulation can serve as a criterion for distinguishing one state from its neighbor state.

Monitoring fluorescence emission in narrow spectral bands allows the isolation of at least some of the *n* states of the system. An initial steep dependence of Stokes' shifts on the volume fraction of DMSO before saturation (i.e, less than 4–5 vol.%) allows separation of some states of the scheme shown in Fig. 2. Taking into account that for volume fractions less than 4 vol.% of DMSO [2b] the solvation number does not exceed 2, one may assume that for a 1.6 vol.% DMSO mixture with toluene, there is on average a two-stage reaction chain: the first stage is in the band of 410 nm (the fluorescence band in neat toluene (Fig. 3) and the minimum for the phase delay in mixtures (Fig. 5)). The second stage can be associated with the red region at about 510 nm. The linear fit of the differential phase delay (Fig. 6) confirms it, directly giving $k_{-1} = 1.1\ 10^9\ s^{-1}$ by using Eq. (13).

Equation (12), which describes the two-stage scheme, satisfactorily fits the obtained data, giving $k_1 = 2.56\ 10^9\ s^{-1}$ in the basis of modulation coefficient data. This value is in excellent agreement with the bimolecular diffusion–limited rate constant that can be calculated as $k_d = 1.19 \cdot 10^{10}\ l \cdot mol^{-1} \cdot s^{-1}$ from this rate constant (compare with the value that can be determined by viscosity of toluene: $k_d = 1.13 \cdot 10^{10}\ l \cdot mol^{-1} \cdot s^{-1}$ [12]). Unlike for other compositions of binary mixtures, for 0.8 vol.% DMSO the experimental data for 0.8 vol.% DMSO failed to fit properly by Eq. (12).

In principle, two sets of the best-fitting parameters can be obtained using either the expressions for phase delays or their demodulation coefficients. However, the phase delay fittings give significantly larger values of rate constants than those by modulation magnitudes. In this case the discrepancy might be attributed to the fact that by definition the modulation is more robust to devia-

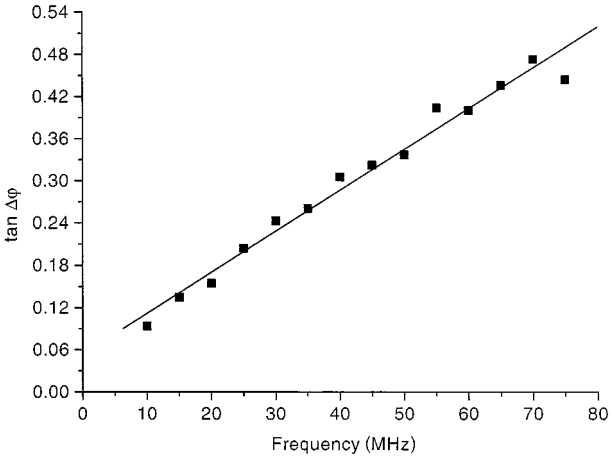

Fig. 6. The plot of tangent of fluorescence phase-angle differential of $\Delta\varphi = (\varphi_2 - \varphi_1)$, where phase angles were measured at $\lambda_2 = 510$ nm and $\lambda_1 = 410$ nm, respectively, versus modulation frequency in a 1.6 vol.% mixture of DMSO with toluene.

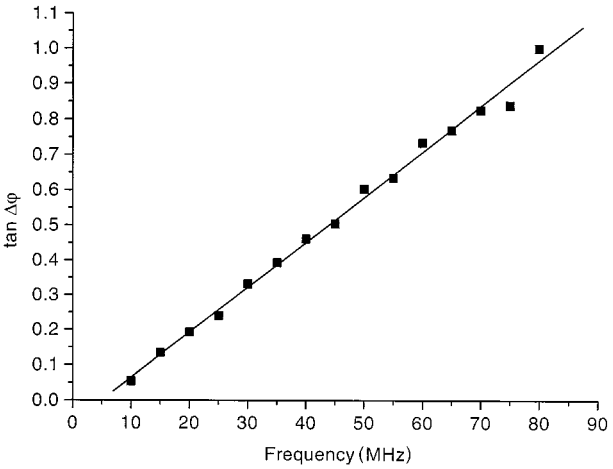

Fig. 7. The plot of tangent of fluorescence phase-angle differential $\Delta\varphi = (\varphi_2 - \varphi_1)$, where phase angles were measured at $\lambda_2 = 560$ nm and $\lambda_1 = 455$ nm, respectively, versus modulation frequency in a 3.2 vol.% mixture of DMSO with toluene.

tions in values of $P_j(\omega)$ and $Q_j(\omega)$ than $\tan \varphi_j = -Q_j(\omega)/P_j(\omega)$. The latter is a ratio, which for large phase angles results in large number for $\tan \varphi_j$, if $P_j(\omega)$ is small. As mentioned earlier, the number of stages can be determined on average only, so that there might be deviations in the values of measured phase angles and demodulations.

The differential phase delay approach also allows the separation of the third and second states in a 3.2 vol.% DMSO mixture in which, according to the results obtained in Ref. 2c, the plausible number of states is three. In a 1.6 vol.% DMSO mixture, the location of the fluorescence peak in a region of 450 nm (see Fig. 3) can be associated with the second state. The dependence of phase delay on fluorescence wavelengths (see Fig. 5, **curve 3**) allows the suggestion that the third state is associated with $\lambda \geq 530$ nm. Equation (13) confirms the linear fit of the differential phase delay between bands at 455 nm and 560 nm for a 3.2% DMSO mixture (Fig. 7) that gives $k_{-2} = 1.4\ 10^9\ s^{-1}$. The rate constants of the decay of solvation complexes k_{-1} and k_{-2} are physically meaningful, that is, equilibrium constants estimated on their basis correspond to the situation in which the equilibrium is well on the side of the solvated dipoles in agreement with experimental facts.

In conclusion, the differential phase delay technique of frequency-domain fluorometry can have an actual advantage over time-domain methods in studying elementary processes of preferential solvation.

ACKNOWLEDGMENTS

The fluorescence probe molecule Py(S)DMA has been synthesized by Dr. W. Kühnle, Max-Planck-Institut, Göttingen. N. Kh. P. thanks the Màx Planck Society for support. The work was also supported by the Russian Foundation for Basic Researches (Grants No. 01-03-32819 and 00-15-97433).

REFERENCES

1. C. Reichardt (1988) *Solvents and Solvent Effects in Organic Chemistry*, 2nd ed., Verlag Chemie, Weinheim; C. Reichardt (1994), *Chem. Rev.* **94**, 2319–2358.
2. (a) N. K. Petrov, A. Wiessner, T. Fiebig, and H. Staerk (1995) *Chem. Phys. Letters* **241**, 127–132; (b) N. K. Petrov, A. Wiessner, and H. Staerk (1998) *J. Chem. Phys.* **108**, 2326–2330; (c) N. K. Petrov, A. Wiessner, and H. Staerk (2001) *Chem. Phys. Lett.*, submitted for publication.
3. (a) F. Cichos, A. Willert, U. Rempel, and C. von Borczyskowski (1997), *J. Phys. Chem. A*, **101**, 8179–8179; (b) F. Cichos, R. Brown, U. Rempel, and C. von Borczyskowski (1999) *J. Phys. Chem. A* **103**, 2506–2512.
4. J. N. Demas (1983) *Excited State Lifetime Measurements*, Academic Press, New York, pp. 50–53.
5. E. Gratton, J. R. Alcala, B. Barbiery (1991) in W. R. G. Baeyens, D. de Keukeleire, and K. Korkidis (Eds.) in *Luminescence Technique in Chemical and Biochemical Analysis*, Marcel Dekker, Inc., New York, pp. 47–72.
6. (a) J. Lakowicz and A. Balter (1982) *Biophys. Chem.* **16**, 99–116; (b) J. R. Lakowicz (1983) *Principles of Fluorescence Spectroscopy*, Plenum, New York. (c) J. R. Lakowicz, I. Gryczynski, G. Laczko, N. Joshi, and M. L. Johnson (1991) in W. R. G. Baeyens, D. de Keukeleire, and K. Korkidis (Eds.), *Luminescence Technique in Chemical and Biochemical Analysis*, Marcel Dekker, Inc., New York, pp. 141–177.
7. K. Nishiyama and T. Okada (1998) *J. Phys. Chem. A* **102**, 9729–9733.
8. E. L. Lippert (1975) in J. B. Birks (Ed.) *Organic Molecular Photophysics*, Vol. 2, John Wiley, New York, pp. 1–29.
9. T. V. Veselova, L. A. Limareva, A. C. Cherkasov, and V. I. Shirokov (1965) *Optics Spectrosc.* **19**, 78–85.
10. A. Morita (1980) *J. Chem. Phys.* **73**, 230–234.
11. G. Weber (1977) *J. Chem. Phys.* **66**, 4081–4091.
12. A. J. Gordon and F. A. Ford (1972) *The Chemist's Companion*, Wiley, New York, pp. 4–16.